

## INFLUENCE OF HYDRAZINE ON THE VIBRATIONAL MODES OF KAOLINITE

C. T. JOHNSTON<sup>1</sup> AND D. A. STONE<sup>2</sup>

<sup>1</sup> Department of Soil Science, University of Florida, Gainesville, Florida 32611

<sup>2</sup> HQ AFESC/RDVS, Tyndall AFB, Florida 32403

**Abstract**—Raman and Fourier-transform-infrared (FTIR) spectroscopic methods and X-ray powder diffraction (XRD) techniques have been used to study the influence of hydrazine on the vibrational modes of kaolinite. Strong vibrational perturbations of the OH-stretching and -deformation bands were observed in the Raman and FTIR spectra on intercalation. The intensities of the Raman- and IR-active OH-stretching bands decreased significantly upon intercalation; the intensities of the Raman bands were reduced to a greater extent than the IR bands. The deformation bands were also strongly perturbed by the presence of hydrazine in the interlamellar region. Upon evacuation of the intercalate, two new bands at 3628 and 912 cm<sup>-1</sup> were noted, indicating the presence of a different structural conformation of the complex under vacuum. Similar results were obtained using XRD, on evacuation of the kaolinite-hydrazine (KH) complex the d(001) value decreased from 10.4 to 9.6 Å. Partial collapse of the intercalate from 10.4 to 9.6 Å was probably due to keying of the -NH<sub>2</sub> moiety of hydrazine into the siloxane ditrigonal cavity, as indicated by a blue-shift of the inner-OH band from 3620 to 3628 cm<sup>-1</sup>. Structural OH vibrational modes may therefore be useful probes of amine interactions with clay mineral surfaces.

**Key Words**—Fourier-transform infrared spectroscopy, Hydrazine, Kaolinite, OH-vibration modes, Raman spectroscopy, X-ray powder diffraction.

### INTRODUCTION

The OH-stretching bands of kaolinite have frequently been used as reporter groups to study the interlayer region. Unlike the broad, poorly resolved OH-stretching bands associated with many 2:1 layer silicates, the five distinct IR- and Raman-active OH-stretching bands of kaolinite are well-resolved and are sensitive to subtle changes in their local environment. Shifts in the position, bandwidth, and relative intensities of the inner-surface-OH-stretching ( $\nu(\text{O-H})$ ) bands of kaolinite reflect changes which occur in the interlamellar environment, and perturbations of these structural  $\nu(\text{O-H})$  bands of kaolinite have been used to obtain information about the degree of structural disorder (Barrios *et al.*, 1977; Brindley *et al.*, 1986), dehydration-dehydroxylation processes (Fripiat and Toussaint, 1963; White *et al.*, 1970; Costanzo and Giese, 1985), the nature of interlayer bonding (Wieckowski and Wiewiora, 1976; Wiewiora *et al.*, 1979), and the structure and bonding of guest species in the interlayer region (Anton and Rouxhet, 1977; Johnston *et al.*, 1984; Thompson and Cuff, 1985; Raupach *et al.*, 1987).

Direct intercalation of kaolinite by guest molecules is restricted to a select group of small polar molecules including dimethyl sulfoxide (DMSO), hydrazine, formamide, and N-methyl formamide (NMF). Other guest species that do not intercalate directly, such as H<sub>2</sub>O or D<sub>2</sub>O, can also be placed in the interlayer region, but only after the clay structure has been expanded. The inner-OH group is located between the silicate tetrahedral and aluminum octahedral layer and is not

accessible to guest species in the interlayer region. Thus, the  $\nu(\text{O-H})$  band of this group at 3620 cm<sup>-1</sup> is not readily perturbed by intercalation reactions.  $\nu(\text{O-H})$  bands from the inner-surface-OH groups, however, which are located on the interlayer surface, are strongly influenced by the presence of intercalated species. Regardless of the intercalation process, the reported vibrational spectra of kaolinite intercalates have three features in common: (1) the intensity of the inner-surface  $\nu(\text{O-H})$  bands are less than their non-intercalated values; (2) a set of "new" bands is present at lower frequencies compared with the unperturbed  $\nu(\text{O-H})$  bands; and (3) the position and integrated intensity of the inner-OH-stretching band at 3620 cm<sup>-1</sup> are not influenced by the intercalation process. The first two observations result from the formation of intermediate-strength hydrogen bonds between the inner-surface-OH groups and the interlayer guest species, which shift the inner-surface  $\nu(\text{O-H})$  bands to lower frequencies. The third observation is due to the inability of the inner-OH group to interact with the intercalated species due to its inaccessible location (Ledoux and White, 1964; Olejnik *et al.*, 1968; Johnston *et al.*, 1984).

Intercalation of kaolinite by hydrazine has been used recently by several research groups to examine the interlayer surface of kaolinite over different time scales. Thompson's <sup>29</sup>Si nuclear magnetic resonance study (1985) of several kaolinite intercalates, including the KH complex, showed that hydrazine was responsible for a shift of the <sup>29</sup>Si resonance from  $\delta = 91.5$  to  $\delta = 92.0$ . This shift is indicative of a reduction in the electron-withdrawing effect of the inner-surface-OH groups

on the siloxane tetrahedra. In a similar capacity, hydrazine was used to induce artificial disorder in kaolinite (Barrios *et al.*, 1977; Thompson and Barron, 1987); artificial  $\pm b/3$  stacking faults were produced in kaolinite by intercalation with, and subsequent removal of, hydrazine. At present, little is known about the bonding mechanisms of hydrazine to the interlayer surface of kaolinite.

The present study examined the influence of hydrazine on the stretching and deformation modes of the OH groups of kaolinite through the combined application of Raman and Fourier-transform infrared (FTIR) spectroscopy. The selection rules for allowed vibrational transitions in Raman and IR spectroscopy are different; thus, a more complete understanding about the interaction of hydrazine with the interlayer surface of kaolinite can be obtained by combined application of these two methods. In addition, FTIR spectroscopy is characterized by an intrinsically greater sensitivity and resolution for surface studies compared with dispersive-IR methods (Bell, 1980; Griffiths and de-Haseth, 1986; Bell, 1987). Although the sensitivity of Raman spectroscopy is much less than that of FTIR, water is less Raman-active than IR-active; thus, the Raman spectra of clay minerals can readily be obtained in aqueous suspension (Johnston *et al.*, 1985).

In an earlier dispersive-IR study of the KH complex, Ledoux and White (1966) observed that the inner-surface  $\nu(\text{O-H})$  bands were strongly influenced by the presence of hydrazine and that the inner-OH  $\nu(\text{O-H})$  band at  $3620\text{ cm}^{-1}$  was not affected. Their IR data, however, were limited to spectral observations  $>2500\text{ cm}^{-1}$ , which did not permit the lower-frequency OH-deformation modes,  $\delta(\text{O-H})$ , to be examined. Changes in the position and intensity of the OH-deformation bands ( $\delta(\text{O-H})$ ) of kaolinite, observed in the  $900\text{--}1000\text{-cm}^{-1}$  region, should correlate well with the behavior of the  $\nu(\text{O-H})$  intercalate bands and thus provide additional insight into interactions of guest species with the mineral surface. A similar approach was used to study the IR-active  $\delta(\text{O-H})$  modes of montmorillonite, in order to probe the behavior of water on reduced-charge smectite surfaces exchanged with different metal cations (Sposito *et al.*, 1983). Insofar as we are aware, lower-frequency IR or Raman data have not been reported for the KH complex. The scope of this paper is restricted to perturbations of kaolinite induced by the presence of hydrazine. The perturbed vibrational modes of the intercalated hydrazine species will be reported elsewhere.

## EXPERIMENTAL

The sample studied was kaolinite KGa-1 collected from Washington County Georgia, obtained from the Source Clays Repository of The Clay Minerals Society. A complete description of the physical properties of this clay sample was given by van Olphen and Fripiat

(1979). In addition, Raman and IR spectra of this clay have been reported (Johnston *et al.*, 1984; Johnston *et al.*, 1985). A dilute aqueous suspension of the kaolinite sample containing  $<2.0\text{-}\mu\text{m}$  equivalent spherical diameter (e.s.d.) particles was prepared by suspending 0.1 g of oven-dry kaolinite in 100 ml of distilled-deionized water. The clay suspension was dispersed by adjusting the pH of the suspension to 9.2 by addition of small aliquots of 0.01 M NaOH. The kaolinite suspension was size-fractionated immediately by centrifugation, and the fraction having an e.s.d. of  $<2.0\text{ }\mu\text{m}$  was collected. The suspension was then flocculated by adjusting the pH to 6.0 using a few drops of 0.01 M HCl. A small aliquot of the size-fractionated clay suspension was dried on a  $25\text{ mm} \times 2\text{ mm}$  ZnSe disk. The disk was mounted in a controlled-environment 10-cm pathlength gas cell in the sample compartment of an FTIR spectrometer. The controlled-environment gas cell was connected to a vacuum/gas manifold, with pressures within the cell being measured using a combination of Penning and Pirani gauges. The sample compartment, transfer optics, and interferometer of the FTIR spectrometer were evacuated to 0.05 torr to eliminate interferences from atmospheric  $\text{CO}_2$  and  $\text{H}_2\text{O}$  vapor. Anhydrous hydrazine (Reg. No. 302-01-2) obtained from Aldrich Chemical Company (98% purity) was used without further purification.

IR spectra were obtained on a Bomem DA3.10 Fourier-transform IR spectrometer. The DA3.10 spectrometer incorporates a Michelson interferometer with the beamsplitter positioned at a  $30^\circ$  angle to the optical axis. The mercury-cadmium-telluride (MCT) detector used in this investigation had a measured  $D^*$  value of  $3.13 \times 10^9\text{ cmHz}^{0.5}$  and a low-frequency cutoff of  $400\text{ cm}^{-1}$  ( $25\text{ }\mu\text{m}$ ). The optical resolution ranged between 1.0 and 0.5 wavenumbers. A comparison of several spectra obtained using resolution values of 2.0, 1.0, and  $0.5\text{ cm}^{-1}$  showed that the spectra were not instrument-limited for nominal resolution values of 0.5 and  $1.0\text{ wavenumbers}$ ; the  $2.0\text{-wavenumber}$  spectrum was, however, instrument-limited. The Bomem DA3.10 spectrometer was controlled through a general-purpose-interface-bus (IEEE-488) interface to a DEC Vaxstation-II computer.

Raman spectra were collected on a Spex 1403 3/4 m double monochromator interfaced to a Nicolet 1180E computer, controlled through an Apple Macintosh Plus computer. The 488-nm line of an argon ion laser (Spectra Physics 171) was used at an incident-power output of 100 mW measured at the sample. For the Raman measurements, a small amount of kaolinite was placed in a glass capillary tube, followed by the addition of hydrazine. The capillary tube was then sealed and allowed to stand for 48 hr. Raman spectra were obtained using a  $90^\circ$  back-scattering collection geometry. The spectral slit width ranged from  $2\text{ to }1\text{ cm}^{-1}$ . X-ray powder diffraction (XRD) patterns were obtained using

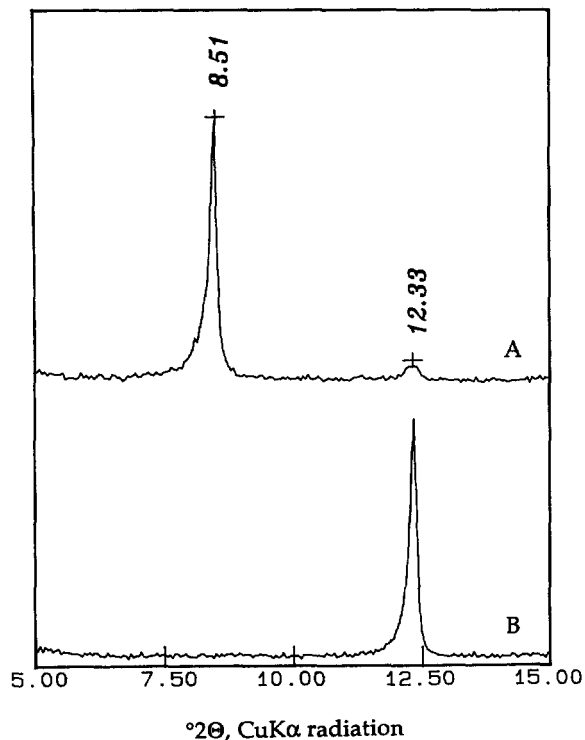


Figure 1. X-ray diffraction patterns of (A) a kaolinite-hydrazine intercalate, and (B) non-intercalated KGa-1 kaolinite at 1 atm pressure and 298 K.

a Nicolet computer-controlled system equipped with a stepping-motor accuracy of  $0.0025^\circ 2\theta$ . Samples were scanned at  $2^\circ 2\theta/\text{min}$ , using  $\text{CuK}\alpha$  radiation. The XRD patterns were collected in an "open" atmosphere. After the samples had equilibrated for a minimum of 1 hr in a vacuum chamber, they were quickly removed and mounted on the open sample stage. XRD patterns were typically collected within 15 min of removal from the vacuum chamber. The rate of hydrazine intercalation into kaolinite was determined by placing a few drops of hydrazine on a kaolinite sample mounted on the X-ray diffractometer. XRD patterns were collected every 15 min.

## RESULTS AND DISCUSSION

Immersion of kaolinite into a solution containing hydrazine for 24 hr resulted in the formation of a stable KH intercalation complex. XRD patterns showing the 001 reflections of kaolinite and of the KH intercalate at 1 atm pressure and  $25^\circ\text{C}$  are presented in Figure 1. The observed  $8.51^\circ 2\theta$  001 reflection of the KH intercalate (Figure 1B) corresponds to a  $d(001)$  value of  $10.4 \text{ \AA}$ , an observed increase in the interlayer spacing of  $3.24 \text{ \AA}$  compared with the value of  $7.16 \text{ \AA}$  for non-intercalated kaolinite (Figure 1A). The well-defined, relatively sharp  $8.51^\circ 2\theta$  001 reflection in the XRD

pattern of the KH complex obtained at 1 atm and 298 K (Figure 1B) suggests that the KH complex was fairly well ordered under these conditions. Furthermore, the negligible intensity of the  $12.33^\circ 2\theta$  reflection in the XRD pattern (Figure 1B) indicates that intercalation was essentially complete and that very little non-intercalated kaolinite remained. The observed  $d(001)$  values of  $10.4 \text{ \AA}$  of the KH intercalation complex is in good agreement with the reported literature value of  $10.4 \text{ \AA}$  (Weiss *et al.*, 1963; Ledoux and White, 1966; Barrios *et al.*, 1977).

The amount of hydrazine sorbed by kaolinite at 1 atm pressure and 298 K ranged between 2 and 4 hydrazine molecules per unit cell of kaolinite. The gravimetric analysis, however, was not capable of distinguishing between hydrazine intercalated into the structure and that physically adsorbed on the external surfaces or within micropores. Similar values were measured in related thermal decomposition studies of the kaolinite-dimethylsulfoxide (DMSO) complex (Adams and Wautl, 1980; Breen and Lynch, 1988), in which the reported weight loss for a kaolinite-DMSO complex was 19% on heating to  $220^\circ\text{C}$ , corresponding to 1.5 DMSO molecules intercalated per unit cell of kaolinite. On evacuation of the KH complex, the number of hydrazine molecules remaining in the intercalate was reduced to 0.5 hydrazine molecules per unit cell. This reduced pressure loading corresponds to one hydrazine molecule per siloxane ditrigonal cavity.

The rate of hydrazine intercalation into kaolinite is shown by a plot of the XRD 001 intensities of kaolinite and of the KH complex vs. time after initial immersion of the kaolinite into liquid hydrazine (Figure 2). On exposure to hydrazine, the intensity of the non-intercalated 001 reflection at  $12.33^\circ 2\theta$  ( $7.16 \text{ \AA}$ ) decreased, and the 001 reflection increased to  $10.4 \text{ \AA}$  ( $8.51^\circ 2\theta$ ) for the KH complex. The increase in intensity of the 001 reflection at  $8.51^\circ 2\theta$  indicates that the intercalation reaction was about complete after 2 hr. The sharp decrease in intensity of the non-intercalated 001 reflection at  $12.33^\circ 2\theta$  (Figure 2), however, suggests that the intercalation process may have reached completion in as little as 30 min.

FTIR and Raman spectra of the KH complex (bottom) and of non-intercalated kaolinite (top) in the  $3600\text{--}3725 \text{ cm}^{-1}$  region at 1 atm of pressure are shown in Figure 3. On intercalation, the intensities of the Raman-active (Figure 3B)  $3652\text{--}$ ,  $3668\text{--}$ ,  $3688\text{--}$ , and  $3695\text{--}\text{cm}^{-1}$  bands were strongly reduced. In contrast, the intensity of the  $3620\text{--}\text{cm}^{-1}$  band was not affected by intercalation (Figure 3B, bottom). A similar result was observed in the IR spectra of the KH complex (Figure 3A); the intensity and position of the  $3620\text{--}\text{cm}^{-1}$  band in the IR spectrum of the KH complex did not change significantly on intercalation. The intensities of the  $3652\text{--}$ ,  $3668\text{--}$ , and  $3695\text{--}\text{cm}^{-1}$  bands, however, were reduced significantly by the presence of hydrazine (Fig-

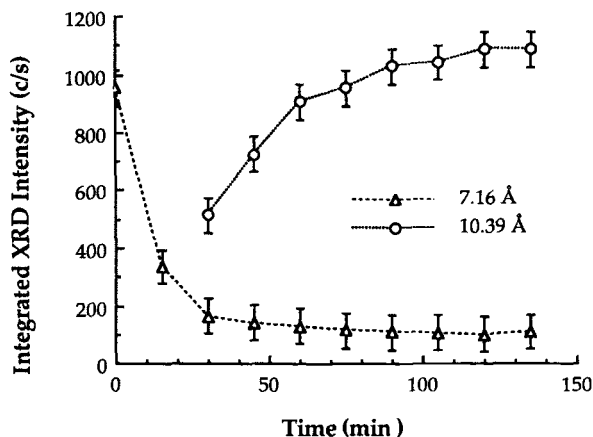


Figure 2. Plot of the integrated intensities of the 001 reflections of non-intercalated kaolinite ( $12.3^{\circ}2\theta$ , 7.16 Å), and of the kaolinite-hydrazine complex ( $8.5^{\circ}2\theta$ , 10.39 Å) vs. time after initial exposure to hydrazine.

ure 3A, bottom). The Raman and FTIR spectra of the KH complex differed in that the Raman intensities of the 3652-, 3668-, and 3688-, and 3694- $\text{cm}^{-1}$  bands were negligible after intercalation, whereas the IR bands in this region maintained significant intensity. A qualitatively similar result was observed for the kaolinite-DMSO complex, in that the IR-active  $\nu(\text{O-H})$  bands maintained significant intensity after intercalation. The positions of the residual  $\nu(\text{O-H})$  bands observed in the IR spectrum (Figure 3A, bottom) were also different after intercalation. Although the 3695- and 3652- $\text{cm}^{-1}$  bands were still present, the 3668- $\text{cm}^{-1}$  band was no longer discernable in the IR spectrum of the intercalate. In addition, the width of the intercalated 3652- and 3695- $\text{cm}^{-1}$  bands of the KH intercalate were larger than those observed for non-intercalated kaolinite (Johnston *et al.*, 1985).

FTIR spectra of the KH complex in the 3600–3725  $\text{cm}^{-1}$  region are shown in Figure 4 for 1 atm pressure (Figure 4A, top spectrum) and for several reduced-pressure values. On evacuation, a new, higher-frequency band appeared at 3628  $\text{cm}^{-1}$  and increased in intensity at the expense of the 3620- $\text{cm}^{-1}$  band as a function of pressure. A similar shift in frequency of the inner-OH-stretching band induced by a guest intercalate has not been reported previously. There is little doubt regarding the assignment of the 3628- $\text{cm}^{-1}$  band to the inner-OH group, because of the strong intensity borrowing between the 3620- and 3628- $\text{cm}^{-1}$  bands. The presence of two discrete inner-OH-stretching bands indicated that a different structural conformation of the intercalation complex was induced as the pressure was decreased. A similar result was not observed in the Raman spectra of the KH complex, where a single band at 3620  $\text{cm}^{-1}$  was observed due to the fact that the Raman spectra were obtained at 1 atm pressure.

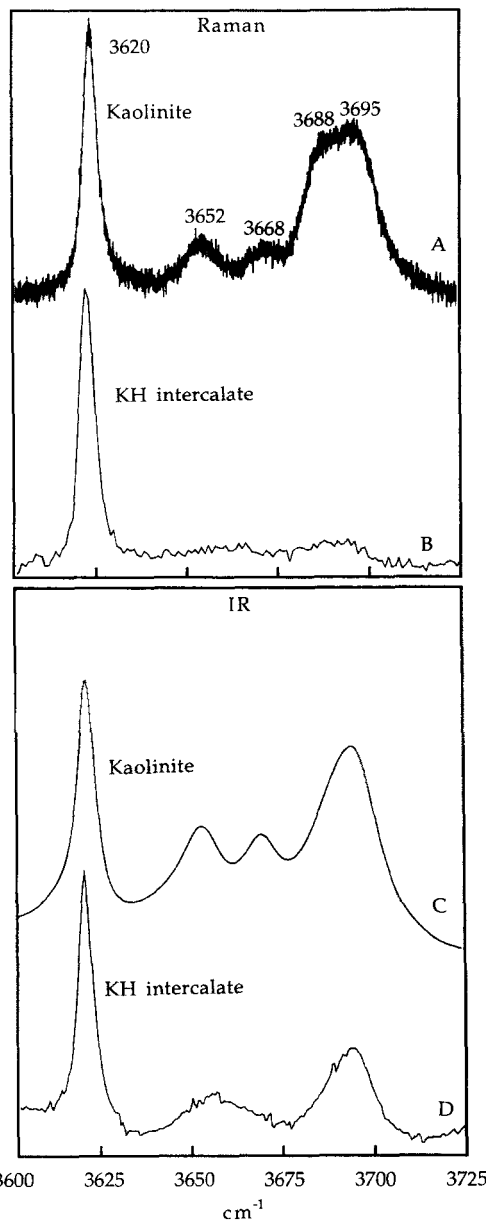


Figure 3. Raman (top) and Fourier-transform infrared (bottom) spectra of non-intercalated kaolinite (spectra A and C), and of kaolinite-hydrazine intercalates (spectra B and D) at 298 K and 1 atm pressure.

Similar results were observed in the OH-deformation region ( $\delta(\text{O-H})$ ) of the KH intercalate. The  $\delta(\text{O-H})$  bands were influenced strongly by the presence of hydrazine. For comparison, the FTIR spectrum of non-intercalated kaolinite in the  $\delta(\text{O-H})$  region of kaolinite is shown at the top of Figure 5; the 915- and 940- $\text{cm}^{-1}$  bands have been assigned to the inner-surface-OH and inner-OH groups, respectively (Rouxhet *et al.*, 1977). The band observed at 957  $\text{cm}^{-1}$  (Figure 4E) can be

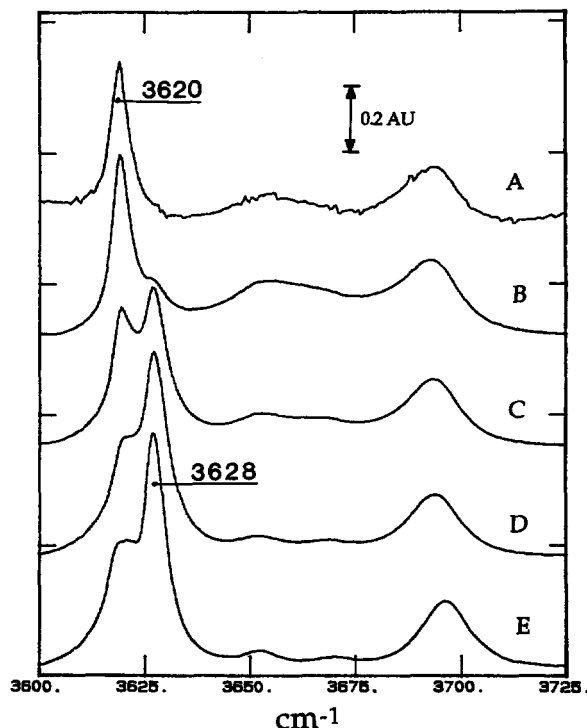


Figure 4. Controlled-environment Fourier-transform infrared spectra of a kaolinite-hydrazine complex obtained as a function of pressure at 298 K. Pressure values corresponding to each spectrum, starting at the top (spectrum A), were 760, 1.0, 0.1, 0.01, 0.001, and  $1.0 \times 10^{-4}$  torr, respectively.

assigned as the  $\nu_{12}$  band of hydrazine (Durig *et al.*, 1966), which corresponds to an  $\text{NH}_2$ -rocking motion. Unfortunately, the  $957\text{-cm}^{-1}$  band obfuscates the inner-OH band at  $940\text{ cm}^{-1}$ . The inner-surface  $\delta(\text{O-H})$  bands, however, are clearly resolved and exhibit a significant blue-shift in frequency from  $904$  to  $912\text{ cm}^{-1}$  on reducing the pressure from 760 to  $10^{-4}$  torr. Under a vacuum of  $10^{-4}$  torr, the  $912\text{-cm}^{-1}$  band was the dominant inner-surface-OH deformation band. An increase in frequency of a deformation band (e.g.,  $\delta[\text{O-H}]$  or  $\delta[\text{N-H}]$ ) was commonly accompanied by a red-shift of the corresponding stretching mode indicative of increased hydrogen bonding (Miyazawa, 1958). Although the inner-OH  $\nu(\text{O-H})$  bands were perturbed on intercalation, changes in the position, shape, and width of the  $\nu(\text{O-H})$  bands showed no consistent trend on evacuation (Figure 4). The clearly resolved blue-shift of the inner-surface  $\delta(\text{O-H})$  bands (Figure 5) indicates that the inner-surface-OH groups formed stronger hydrogen bonds on evacuation. Furthermore, the inner-surface  $\delta(\text{O-H})$  bands in the  $904\text{--}915\text{-cm}^{-1}$  region appear as distinct bands at discrete frequencies of about  $904$  and  $912\text{ cm}^{-1}$ , as opposed to a continuous shift in frequency between these values. The KH spectrum ob-

tained at intermediate pressure (Figure 5C) illustrates clearly the presence of two separate bands, in agreement with results obtained for the OH-stretching region, indicating that two distinct structural conformations of kaolinite are present.

Raman spectra of the KH complex have not been reported previously in the literature; however, the Raman results presented here are qualitatively similar to previously reported IR spectra for the KH complex (Ledoux and White, 1966). The IR spectra of the KH complex in the  $2800\text{--}3800\text{ cm}^{-1}$  region were characterized by the following observations: (1) the position and integrated intensity of the  $3620\text{-cm}^{-1}$  band were not influenced by the presence of hydrazine; (2) the intensities of the  $3652\text{-}$ ,  $3670\text{-}$ , and  $3695\text{-cm}^{-1}$  bands were strongly reduced upon formation of the intercalation complex relative to non-reacted kaolinite; and (3) additional bands at  $3570$ ,  $3470$ ,  $3365$ ,  $3310$ ,  $3200$  and  $2970\text{ cm}^{-1}$  were observed after intercalation (Ledoux and White, 1966). The decreased intensity of the inner-surface-OH-stretching bands and the appearance of a suite of new bands shifted to lower frequencies indicate that the intercalated hydrazine species formed hydrogen bonds with the inner-surface-OH groups of kaolinite.

A ball and stick projection of the kaolinite structure (Figure 6) illustrates two distinct types of OH groups in the kaolinite: inner-OH groups located between the Al octahedral layer and the Si tetrahedral layer, and inner-surface-OH groups located on the basal plane of the Al octahedral layer. Numerous IR studies of kaolinite during the past 30 years have firmly established the assignment of the  $3620\text{-cm}^{-1}$  band to inner-OH groups. Detailed band assignments for the  $3652\text{-}$ ,  $3668\text{-}$ , and  $3688\text{-}$ , and  $3695\text{-cm}^{-1}$  bands have not yet been made. Assignment of these bands to specific OH groups is complicated by several factors, including uncertainty as to the orientation of the inner-surface-OH groups, the presence of naturally occurring stacking faults, and coupling of several of the vibrational modes (Rouxhet *et al.*, 1977). There is little disagreement, however, that the bands of  $3552$ ,  $3668$ ,  $3688$ , and  $3695\text{ cm}^{-1}$  as a group correspond to the  $\nu(\text{O-H})$  vibrations of inner-surface-OH groups (Figure 6).

Inner-surface-OH groups can readily form hydrogen bonds with intercalated species, as shown by the Raman and FTIR spectra of the KH intercalation complex (Figures 3A and 3B). In selective deuteration studies at room temperature of a kaolinite sample previously intercalated with hydrazine, Ledoux and White (1964) and Wada (1967) found that the intensities of the inner-surface-OH-stretching bands at  $3695$ ,  $3670$ , and  $3650\text{ cm}^{-1}$  were replaced by their deuterated counterpart bands at  $2725$ ,  $2710$ , and  $2698\text{ cm}^{-1}$ . Thus, these OH groups were isotopically exchanged with deuterium. In contrast, the inner-OH-stretching band at  $3620\text{ cm}^{-1}$  was not significantly perturbed by the deuteration pro-

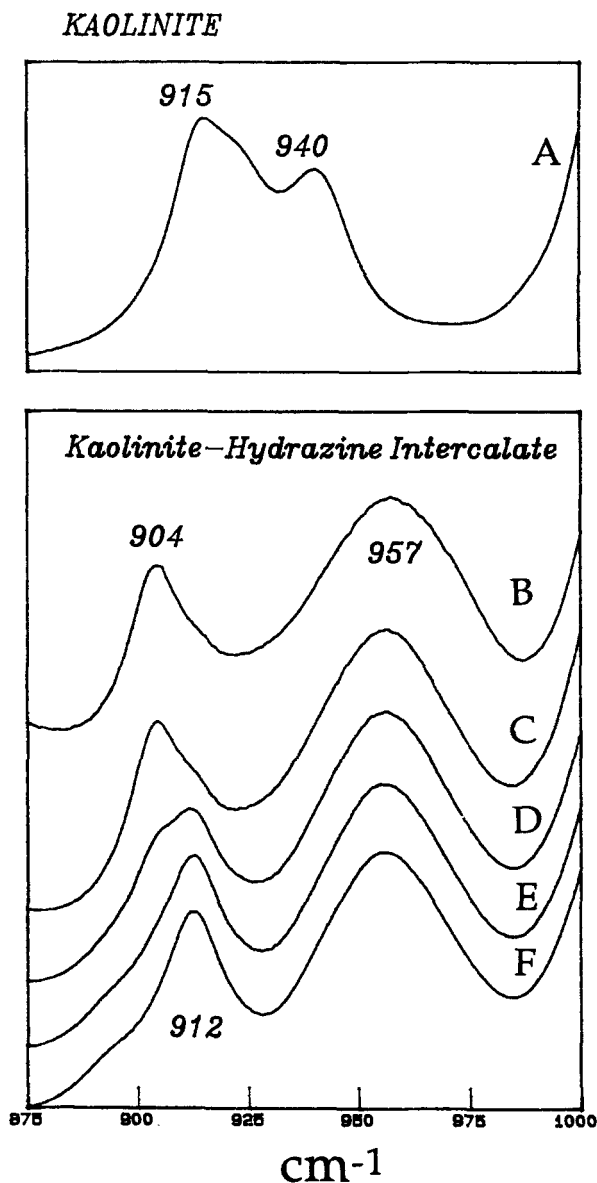


Figure 5. Controlled-environment Fourier-transform infrared spectra of a kaolinite-hydrazine complex obtained as a function of pressure at 298 K. Pressure values corresponding to each spectrum, starting at the spectrum B were 760 (B), 1.0 (C), 0.01 (D), 0.001 (E), and  $<1.0 \times 10^{-4}$  torr (F), respectively. Spectrum of non-intercalated kaolinite is shown at the top (spectrum A).

cess because of the inaccessible location of the inner-OH group to interact with  $D_2O$ .

Similar behavior has been reported in IR and Raman studies of kaolinite intercalation complexes. Upon intercalation by small polar molecules, the inner-surface-OH-stretching bands were shifted to lower frequencies by 100 to 200  $cm^{-1}$ , due to the formation of hydrogen bonds between the inner-surface-OH groups and the

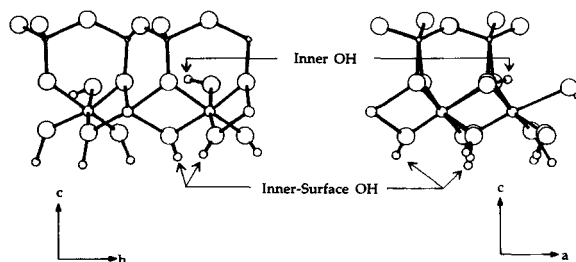


Figure 6. Projection of the kaolinite structure showing the position of the inner OH and inner-surface-OH groups of kaolinite. Atomic coordinates were obtained from Suitch and Young (1983).

guest species (Ledoux and White, 1966; Johnston *et al.*, 1984; and Raupach *et al.*, 1987). The inner-OH group, however, did not participate directly in the formation of hydrogen bonds because of its recessed location (Ledoux and White, 1964). In contrast to the reactive nature of the inner-surface-OH groups, the inner-OH group is characterized by pronounced resistance to isotopic exchange with deuterium and to dehydroxylation. In numerous IR studies of kaolinite intercalates, neither the intensity nor the frequency of the  $3620\text{-}cm^{-1}$  band changed on intercalation (Ledoux and White, 1966; Johnston *et al.*, 1984). Recently, however, Raupach *et al.* (1987) observed a splitting of the  $3620\text{-}cm^{-1}$  band into two components at 3627 and  $3593\text{-}cm^{-1}$  for the dimethylselenoxide intercalate. Isotopic exchange of the inner-OH group with deuterium has been observed, but only at temperatures  $>150^\circ C$  (White, 1968; White *et al.*, 1970). In a related study, Maiti and Freund (1981) showed by direct-current proton conductivity and thermal-IR methods that delocalization of the inner-OH group of kaolinite occurs at temperatures  $>200^\circ C$ .

As the ball and stick projection of kaolinite illustrates (Figure 6), the inner-OH group resides between the Si tetrahedral and Al octahedral layers and is not accessible by most interlamellar species. The fact that hydrazine perturbed the stretching frequency of the inner-OH group suggests that the  $-NH_2$  moiety keyed into the kaolinite surface, resulting in a slight electrostatic repulsion between the  $-NH_2$  and  $-OH$  groups, giving rise to the  $8\text{-}cm^{-1}$  blue-shift. Considering the crystal structure of kaolinite, the inner-OH group can only be approached by a guest molecule small enough to penetrate into or through the siloxane ditrigonal cavity. A space-filling 001 projection of the siloxane ditrigonal cavity of kaolinite constructed using van der Waals atomic radii (Figure 7) illustrates the relative size of hydrazine compared with the ditrigonal hole.

To confirm the hypothesis that hydrazine keyed into the siloxane ditrigonal cavity of kaolinite, XRD patterns of the evacuated complex were obtained at re-

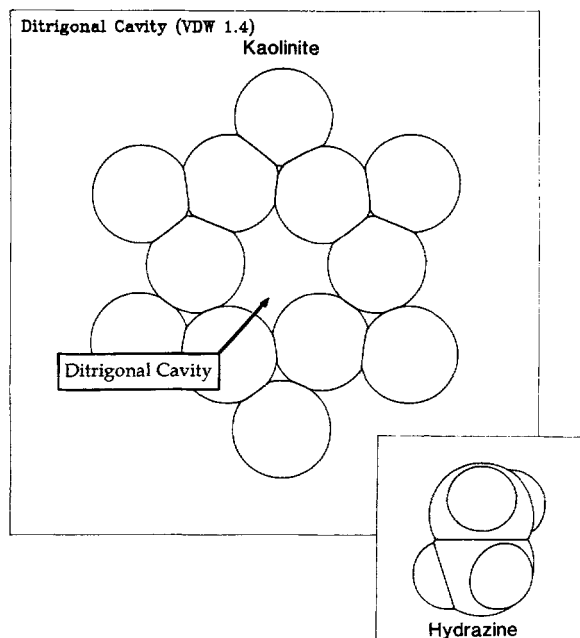


Figure 7. Space-filling 001 projection of the siloxane ditrigonal cavity of kaolinite, shown in relation to a space-filled drawing of hydrazine drawn to the same scale.

duced pressures (Figure 8). The 001 reflections of the KH intercalation complex increased from the 760 torr value of  $8.60^{\circ}2\theta$  ( $10.4\text{ \AA}$ ) to  $9.2^{\circ}2\theta$  ( $9.6\text{ \AA}$ ) at  $10^{-5}$  torr. Thus, the height of the interlamellar region decreased from 3.23 to 2.44  $\text{\AA}$ . This observed decrease in the interlamellar spacing of the KH complex provides conclusive evidence that a structural change of the KH complex did occur on evacuation. This structural change is also reflected in the novel blue-shift of the inner-OH-stretching band from 3620 to 3628  $\text{cm}^{-1}$ , which suggests that the  $-\text{NH}_2$  moiety of the guest hydrazine species was brought into closer contact with the inner-OH group on evacuation. These inner-OH  $\nu(\text{O-H})$  bands at 3620 and 3628  $\text{cm}^{-1}$  are discrete, an additional indication of two different phases.

Similar results were observed in the OH-deformation region; the inner-surface  $\delta(\text{O-H})$  bands showed two discrete bands at 904 and 912  $\text{cm}^{-1}$  on evacuation, indicative of two different structures. The  $d(001)$  value of the KH complex obtained as a function of pressure, however, gradually decreased with evacuation. Probably, two phases were present having 9.6- and 10.4- $\text{\AA}$  spacings, respectively, consistent with the appearance of two discrete bands in the FTIR spectrum. At high surface coverages of hydrazine in the interlamellar region ( $>1$  hydrazine molecule per unit cell), the guest hydrazine species apparently served as molecular props between the siloxane and Al-O-OH layers of kaolinite, resulting in a 10.4- $\text{\AA}$  d-value. On partial loss of hydrazine by evacuation, the intercalated hydrazine

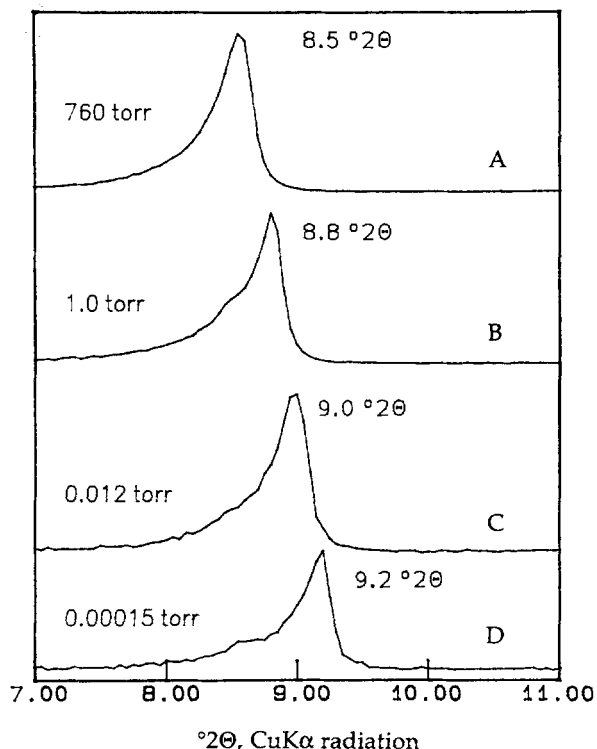


Figure 8. Controlled-environment X-ray powder diffraction patterns of a kaolinite-hydrazine intercalate, obtained as a function of pressure at 298 K.

species keyed into the ditrigonal holes, and the d-value of the complex was reduced to 9.6  $\text{\AA}$ . Similar results have been reported by Costanzo *et al.* (1982, 1984), and Costanzo and Giese (1985), who have observed reduced d-values for kaolinite hydrates heated under mild conditions.

#### SUMMARY AND CONCLUSIONS

Raman and FTIR spectra of the KH complex in the OH-deformation and -stretching regions both showed a strong reduction in intensity for vibrations associated with the inner-surface-OH groups on intercalation. This reduction in intensity resulted from the formation of hydrogen bonds between the inner-surface-OH groups of kaolinite and the interlayer hydrazine species. XRD patterns of the KH complex suggest that the height of the interlamellar region increased by 3.14  $\text{\AA}$  at 1 atm of pressure to accommodate the guest intercalate. As the pressure was reduced, however, this value decreased to 2.44  $\text{\AA}$  and the FTIR spectra showed clearly the presence of a new, higher-frequency inner-OH-stretching band at 3628  $\text{cm}^{-1}$ . In addition, a new OH-deformation band at 912  $\text{cm}^{-1}$  was observed. These results suggest that a structural change of the KH complex occurred at reduced pressure and that the  $-\text{NH}_2$  moiety of hydrazine was brought into close contact

with the inner-OH group through the siloxane ditrigonal cavity. The Raman- and IR-active OH-stretching and -deformation modes of kaolinite appear to be sensitive probes of the interaction between hydrazine molecules and the kaolinite surface.

#### ACKNOWLEDGMENTS

We thank D. L. Bish, R. Próst, and Rasik Raythatha for valuable discussions of the XRD data. This work was supported, in part, by the Environmental Sciences Branch of the United States Air Force. Florida Agricultural Experiment Station Journal Series No. 9413.

#### REFERENCES

- Adams, J. M. and Waltl, G. (1980) Thermal-decomposition of a kaolinite dimethylsulfoxide intercalate: *Clays & Clay Minerals* **28**, 130–134.
- Anton, O. and Rouxhet, P. G. (1977) Note on the intercalation of kaolinite, dickite, and halloysite by dimethylsulfoxide: *Clays & Clay Minerals* **25**, 259–263.
- Barrios, J., Plançon, A., Cruz, M. I., and Tchoubar, C. (1977) Qualitative and quantitative study of stacking faults in a hydrazine-treated kaolinite. Relationship with the infrared spectra: *Clays & Clay Minerals* **25**, 422–429.
- Bell, A. T. (1980) Applications of Fourier-transform infrared spectroscopy to studies of adsorbed species: in *Vibrational Spectroscopies for Adsorbed Species*, A. T. Bell and M. L. Hair, eds., Amer. Chem. Soc. Sympos. Series **137**, American Chemical Society, Washington, D.C., 13–35.
- Bell, A. T. (1987) Infrared spectroscopy of high-area catalytic surfaces: in *Vibrational Spectroscopy of Molecules on Surfaces*, J. T. Yates and T. E. Madey, eds., Plenum Press, New York, 105–134.
- Breen, C. and Lynch, S. (1988) Reexamination of the kinetics of the thermal desorption of dimethylsulfoxide and N-methyl-formamide from a Greensplatt kaolinite: *Clays & Clay Minerals* **36**, 19–24.
- Brindley, G. W., Kao, C., Harrison, J. L., Lipsicas, M., and Raythatha, R. (1986) Relation between structural disorder and other characteristics of kaolinites and dickites: *Clays & Clay Minerals* **34**, 239–249.
- Costanzo, P. M., and Giese, R. F. (1985) Dehydration of synthetic hydrated kaolinites: A model for the dehydration of hallosite(10A): *Clays & Clay Minerals* **33**, 415–423.
- Costanzo, P. M., Giese, R. F., and Lipsicas, M. (1984) Static and dynamic structures of water in hydrated kaolinites. I. The static structure: *Clays & Clay Minerals* **32**, 419–428.
- Costanzo, P. M., Giese, R. F., Lipsicas, M., and Straley, C. (1982) Synthesis of a quasi-stable kaolinite and heat-capacity of interlayer water: *Nature* **296**, 549–551.
- Durig, J. R., Bush, S. F., and Mercer, E. E. (1966) Vibrational spectrum of hydrazine-d<sub>4</sub> and a Raman study of hydrogen bonding in hydrazine: *J. Chem. Phys.* **44**, 4238–4247.
- Fripiat, J. J. and Toussaint, F. (1963) Dehydroxylation of kaolinite. II. Conductometric measurements and infrared spectroscopy: *J. Phys. Chem.* **67**, 30–36.
- Griffiths, P. R. and deHaseth, J. A. (1986) *Fourier-Transform Infrared Spectrometry*: Wiley, New York, 656 pp.
- Johnston, C. T., Sposito, G., and Birge, R. R. (1985) Raman spectroscopic study of kaolinite in aqueous suspension: *Clays & Clay Minerals* **33**, 483–489.
- Johnston, C. T., Sposito, G., Bocian, D. F., and Birge, R. R. (1984) Vibrational spectroscopic study of the interlamellar kaolinite-dimethylsulfoxide complex: *J. Phys. Chem.* **88**, 5959–5964.
- Ledoux, R. L., and White, J. L. (1964) Infrared study of selective deuteration of kaolinite and halloysite at room temperature: *Science* **145**, 47–49.
- Ledoux, R. L. and White, J. L. (1966) Infrared studies of hydrogen bonding interaction between kaolinite surfaces and intercalated potassium acetate, hydrazine, formamide, and urea: *J. Colloid and Interface Sciences* **21**, 127–152.
- Maiti, G. C. and Freund, F. (1981) Dehydration-related proton conductivity in kaolinite: *Clay Miner.* **16**, 395–413.
- Miyazawa, T., Shimanouchi, T., and Mizushima, S. (1958) Normal vibrations of N-methylacetamide: *J. Chem. Phys.* **29**, 611–616.
- Olejnik, S., Aylmore, L. A. G., Posner, A. M., and Quirk, J. P. (1968) Infrared spectra of kaolin mineral-dimethyl sulfoxide complexes: *J. Phys. Chem.* **72**, 241–249.
- Raupach, M., Barron, P. F., Thompson, J. G. (1987) Nuclear magnetic resonance, infrared, and X-ray powder diffraction study of dimethylsulfoxide and dimethylselenoxide intercalates with kaolinite. *Clays & Clay Minerals* **35**, 208–219.
- Rouxhet, D. G., Samudacheata, N., Jacobs, H., and Anton, O. (1977) Attribution of the OH-stretching bands of kaolinite: *Clay Miner.* **12**, 171–178.
- Sposito, G., Prost, R., and Gaultier, J. P. (1983) Infrared spectroscopic study of adsorbed water on reduced-charge Na/Li montmorillonites: *Clays & Clay Minerals* **31**, 9–16.
- Suitch, P. R. and Young, R. A. (1983) Atom positions in highly ordered kaolinite: *Clays & Clay Minerals* **31**, 357–366.
- Thompson, J. G. (1985) Interpretation of solid state <sup>13</sup>C and <sup>29</sup>Si nuclear magnetic resonance spectra of kaolinite intercalates: *Clays & Clay Minerals* **33**, 173–180.
- Thompson, J. G. and Barron, P. F. (1987) Further consideration of the <sup>29</sup>Si nuclear magnetic resonance spectrum of kaolinite: *Clays & Clay Minerals* **35**, 38–42.
- Thompson, J. G. and Cuff, C. (1985) Crystal structure of kaolinite: dimethylsulfoxide intercalate: *Clays & Clay Minerals* **33**, 490–500.
- van Olphen, H. and Fripiat, J. J. (1979) *Data Handbook for Clay Materials and other Non-metallic Minerals*, Pergamon Press, Oxford, 346 pp.
- Wada, K. (1967) A study of hydroxyl groups in kaolin minerals utilizing selective-deuteration and infrared spectroscopy: *Clay Miner.* **7**, 51–61.
- Weiss, A., Thielepape, W., Goring, G., Ritter, W., and Schaffer, H. (1963) Kaolinit Einlagerungs-Verbindungen: in *Proc. Intl. Clay Conf. Stockholm Vol. 1*, I. Th. Rosenqvist and P. Graff-Petersen, eds. Pergamon Press, Oxford, 287–305.
- White, J. L. (1968) Proton migration in kaolinite: *9th Intl. Congr. of Soil Sci. Trans.* 701–707.
- White, J. L., Laycock, A., and Cruz, M. I. (1970) Infrared studies of proton delocalization in kaolinite: *Bull. Groupe. Franc. Argiles* **22**, 157–165.
- Wieckowski, T. and Wiewiora, A. (1976) New approach to the problem of the interlayer bonding in kaolinite: *Clays & Clay Minerals* **24**, 219–223.
- Wiewiora, A., Wieckowski, T., and Sokolowska, A. (1979) The Raman spectra of kaolinite sub-group minerals and of pyrophyllite: *Archiwum Mineralogiczne* **35**, 5–14.

(Received 29 August 1988; accepted 2 May 1989; Ms. 1822)